

Thermoelectric properties of a nanocontact made of two-capped single-wall carbon nanotubes calculated within the tight-binding approximation

Keivan Esfarjani and Mona Zebarjadi

Department of Physics, Sharif University of Technology, Tehran 11365-9161, Iran

Yoshiyuki Kawazoe

IMR, Tohoku University, Sendai 980-8577, Japan

(Received 1 October 2005; revised manuscript received 23 November 2005; published 9 February 2006)

Thermoelectric properties of a nanocontact made of two capped single wall carbon nanotubes (SWCNT) are calculated within the tight-binding approximation and by using Green's function method. It is found that doped semiconducting nanotubes can have high Seebeck coefficients. This in turn leads to very high figures of merit (ZT) for p -doped tubes which turn out to have also a large electrical to thermal conductivity ratio. Transport in the nanocontact device is dominated by quantum interference effects, and thus it can be tuned by doping (charge transfer and/or impurity potential) or application of a (nano-)gate voltage, or a magnetic field. Another reason for high ZT in this device is the absence of phonon transport as there is barely a contact.

DOI: [10.1103/PhysRevB.73.085406](https://doi.org/10.1103/PhysRevB.73.085406)

PACS number(s): 72.20.Pa, 73.63.Fg, 73.21.Hb

I. INTRODUCTION

Today's electronic devices are becoming increasingly small and dense. Extraction of the produced heat from them is, therefore, of paramount importance. Materials with high thermoelectric properties, namely the figure of merit, can be used for this purpose, and also for the purpose of power generation.¹ It has been known² that reducing the dimensionality can increase the thermopower. Indeed, in lower dimensions, singular features appear in the density of states (DOS), and this can lead to large variations of the Fermi-energy-dependent conductivity. The Seebeck coefficient or thermopower, being proportional to the logarithmic derivative of the latter can, therefore, become large, and thereby lead to high figures of merit, ZT . As the DOS of metallic wires is smooth near the Fermi level, metals cannot have a large Seebeck coefficient. One-dimensional (1D) semiconductors, for which the variation of the DOS near the Fermi level is very sharp are, therefore, much better candidates for achieving high ZT . The problem with semiconductors being that they can have high thermal conductivity (due to phonons) which can reduce ZT since the former is defined as $ZT = \sigma S^2 T / \kappa$ where σ, S, κ are, respectively, the electrical conductivity, Seebeck coefficient and the thermal conductivity.

Sun *et al.*³ calculated the thermoelectric properties of Bi nanowires within the semiclassical theory, using the relaxation time approximation, anisotropic effective masses and nonparabolicity of the energy dispersion, and found that for appropriate doping, the figure of merit of a 10 nm wide nanowire can reach 1.5 and increases as the wire width is decreased. On the experimental side, Hsu *et al.*⁴ have synthesized alloys containing nanometer size metallic grains embedded in a semiconducting matrix, reaching a ZT of the order of 2.2, implying again the important role of quantum confinement. A ZT value of 2.4 was also observed in Bi_2Te_3 and Sb_2Te_3 superlattices.⁵ On the other hand, Lyo *et al.*⁶ have used the high thermopower of a nanocontact to map out the thermopower profile of a semiconductor substrate by

their scanning thermo electric microscopy (SThem) device. It becomes clear then that the quantum confinement present in nanoscale systems can yield interesting thermoelectric properties which can be used in order to design cooling devices.

In this work, in order to illustrate further the important thermoelectric properties of nanocontacts, we have considered nanocontacts formed of different configurations of two capped single wall carbon nanotubes (SWCNT) of metallic and also semiconducting nature, and have calculated their conductance, thermopower and figure of merit. Previous works on the thermal properties of nanotubes were done on SWCNT mats and bundles⁷⁻⁹ where disorder was created by wall-wall interactions and adsorbed molecules on the walls which also caused charge transfer to or from the tubes. Some of the transport results were interpreted in terms of percolation of electron paths¹⁰ since transport in the semiconducting phase was deduced to be tunneling dominated. Furthermore, it seems that the experimental samples included mostly ropes of metallic SWCNTs, which eventually became semiconducting due to the disorder caused by dopant atoms and tube-tube interactions. In another set up, the Seebeck coefficient has been found to be moderately large at room temperature with enough doping.¹¹ In the present work, we will also find large values for the Seebeck coefficient, but our system is not totally identical to the experiments as it involves a single contact between two ideal semiconductor nanotube tips.

This paper is organized as follows: The model and theory are described in the next section, followed by results and discussions on the conductance, thermopower, validity of the Wiedemann-Franz law and the figure of merit. A simple discussion on the statistical properties of an assembly of such devices put in series and parallel is also included. The paper is ended with a summary and an alternative proposal where such nanocontacts may be realized.

II. MODEL AND THEORY

Some typical configurations of two (10,0) semiconducting SWCNT used in our calculations, before and after doing mo-

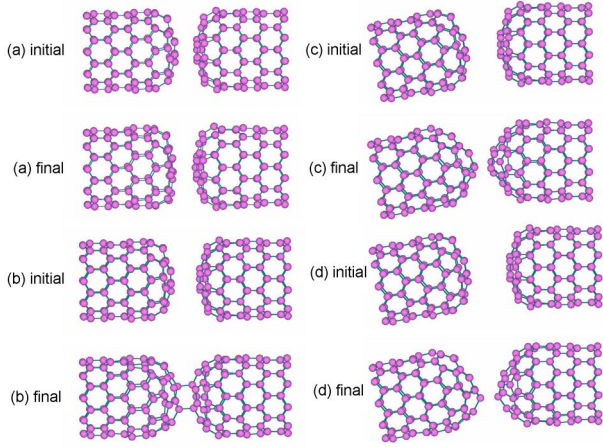


FIG. 1. (Color online) The initial and a typical MD snapshot (called here final) of two semiconducting (10,0) capped nanotubes forming a nanocontact. In order not to take any symmetric configuration, one of the tubes has been rotated and tilted with respect to the other.

lecular dynamics (MD) can be seen in Fig. 1.

To include the effect of vibrations, we have used an adiabatic approximation by taking a configuration average of the transmission coefficient over many (50) uncorrelated snapshots obtained from a molecular dynamics (MD) simulation. The resulting thermoelectric properties were obtained by configuration-averaging the properties calculated from each MD-generated snapshot. A calculation for ideal metallic tubes (not contacts) using the linear response formalism and including electron-phonon interaction in a tight-binding Hamiltonian has also been performed.¹² Their results, however, cannot be compared to the present calculations, since they have studied doped bulk ropes made of metallic single wall carbon nanotubes. In this work, we have neglected the nonadiabatic effects of the electron-phonon interaction. Its effect on transport properties is to reduce the conductance, but the reduction is of the order of tens of percent, (not by an order of magnitude), and therefore, does not affect our conclusions.

In order to calculate the linear transport properties of the nanocontact, the Landauer-Buttiker formula^{13,14} in which the transmission coefficient is calculated by using the Green's function method¹⁵ was used. The formalism is exact in the coherent transport limit where inelastic scattering and phase breaking mechanisms such as electron-phonon interaction are absent. The formulation is within a tight-binding approximation where, for simplicity, only one π orbital was considered for each carbon atom. The effect of the other orbitals forming an sp^2 hybridization (σ bonds) becomes important away from the Fermi energy. The leads are assumed to be continuations of the perfect nanotubes over which it is assumed that there is no voltage or temperature drop. The two-probe Landauer formula can then be used for this purpose. One needs to take the “nanocontact” region long enough so that all potential and temperature drops occur within it. Due to memory and CPU time limitations, we have considered a central region containing 120 atoms. Using infinitesimal voltage and temperature gradient drops across the sample

makes our approximation valid. Within the linear response limit, the thermoelectric properties of a nanosystem can be derived from the definitions of the electrical and thermal currents:^{13,14}

$$I = \frac{2q}{h} \int dE T(E) [f_L(E) - f_R(E)] \quad (1)$$

$$I_Q = \frac{2}{h} \int dE T(E) [f_L(E) - f_R(E)] (E - \mu) \quad (2)$$

where the factor of 2 is for the spin, q is the carrier charge, $T(E)$ is the transmission coefficient of the device, and f_L and f_R are, respectively, the distribution functions of the left and right reservoirs with chemical potentials μ_L and μ_R . In this work, we are interested in the linear response of the system, i.e., we assume that $\Delta\mu = \mu_L - \mu_R$ as well as $\Delta T = T_L - T_R$ are infinitesimally small quantities so that the currents are linear in the latter. Therefore, the chemical potential μ in the thermal current is defined as the average of the left and right chemical potentials. Furthermore the thermoelectric response functions can be obtained from the unperturbed ground state properties of the system.

By using a Taylor expansion in powers of ΔV and ΔT in Eq. (2), the transport properties defined below can easily be expressed in terms of the transmission coefficient $T(E)$

- Conductance : $G = -\frac{I}{\Delta V} \Big|_{\Delta T=0} = q^2 K_0$
 - Peltier Coefficient : $\Pi = \frac{I_Q}{I} \Big|_{\Delta T=0} = K_1 / q K_0$
 - Thermopower : $S = -\frac{\Delta V}{\Delta T} \Big|_{I=0} = K_1 / q T K_0 = \frac{\Pi}{T}$
 - Thermal conductance : $\kappa = -\frac{I_Q}{\Delta T} \Big|_{I=0} = (K_2 - K_1^2 / K_0) / T$
- where K_n is the following integral:

$$K_n = \frac{2}{h} \int dE T(E) \left(-\frac{\partial f}{\partial E} \right) (E - \mu)^n \quad (3)$$

It strongly depends on the analytic properties of $T(E)$ near the Fermi level.

The response of the system is thus defined by the following matrix:

$$\begin{pmatrix} I \\ I_Q \end{pmatrix} = \begin{pmatrix} G & GST \\ \Pi G & T(\kappa + S^2 GT) \end{pmatrix} \begin{pmatrix} -\Delta V \\ -\Delta T/T \end{pmatrix} \\ = \begin{pmatrix} q^2 K_0 & q K_1 \\ q K_1 & K_2 \end{pmatrix} \begin{pmatrix} -\Delta V \\ -\Delta T/T \end{pmatrix} \quad (4)$$

The derivation is trivial and is very similar to the well-known and standard semiclassical one used in textbooks,¹⁶ except that the function $T(E)$ has replaced the energy-dependent Drude conductivity $\sigma(E) = 2 \sum_k v_k v_k \tau_k \delta(E - \epsilon_k)$. To our knowledge the above relations were first derived and discussed by Sivan and Imry.¹⁷

If the transmission function $T(E)$ is analytical, such as in metals, one can use its Taylor expansion around the chemical potential in order to obtain its temperature dependence by using the Sommerfeld expansion. Mott's formula relating the thermopower to the logarithmic derivative of the conductivity in metals, as well as Wiedemann-Franz law expressing the proportionality of the thermal to the electrical conductiv-

ity in metals can be proved by using such an expansion. Finally, the figure of merit is simply given by

$$ZT = \frac{GS^2T}{\kappa} = \frac{K_1^2}{K_2K_0 - K_1^2} \quad (5)$$

Note that, although in the definition of ZT , the full thermal conductance is introduced, in the second part of Eq. (5), we have only put the electronic contribution to κ and the phononic part is omitted. This is a good approximation in metals, but in semiconductors or insulators, the largest contribution to κ is due to phonons. In the considered nanocontact (see Fig. 1), however, since the system is split into two, we do not expect that κ due to phonons would have a significant contribution.

III. RESULTS AND DISCUSSIONS

For the considered nanocontact, as mentioned, we generated uncorrelated configurations from 50 MD snapshots, separated by 10 fs, run at 300 K, for which all the above properties were configuration-averaged. The configurations were generated for two initial separations of the nanotubes denoted by Figs. 1(a) and 1(b). In Fig. 1(a), the initial separation is 2.4 Å, and in Fig. 1(b) it is increased to 3.2 Å (see Fig. 1). After some relaxation time, however, the cap-cap distance is reduced, due to the weak van der Waals interaction between the caps, to a number between 1.7 and 2.2 Å, forming almost a chemical bond. In other runs [Figs. 1(c) and 1(d)], the tubes on each side of the junction were also slightly tilted and rotated so that no accidental symmetry affects the results.

A. Metals versus semiconductors

The calculations were done for both a pair of (5,5) metallic tubes and two pairs of (8,0) and (10,0) semiconducting tubes all at room temperature (in the Fermi-Dirac function in Eq. (3), $k_B T = 0.025$ eV). These results differ in the fact that the interesting features such as large figure of merit (see Fig. 2), occur for chemical potentials near the actual Fermi level of the semiconducting tubes only. So, in what follows, we will focus on the results obtained for the (10,0) tubes.

B. Conductances

In Fig. 3, conductances are compared for the (10,0) tubes placed at two different initial distances and two different orientations. Structure (0,10)-a is clearly in the tunneling regime and structures (0,10)-b and (0,10)-d have stronger coupling as G can be of the order of G_0 for values of the chemical potential away from the gap. The semiconducting gap near energy 0 is apparent, and one can notice very sharp changes in G by 2 or 3 orders of magnitudes within 0.5 eV near the gap. Such large changes are responsible for large Seebeck coefficients, as the latter is the logarithmic derivative (Mott's formula) of the conductance. Although there is still a large variation in the four conductances near the gap, conductances of these four samples are quite different reflecting the mesoscopic character of the considered system.

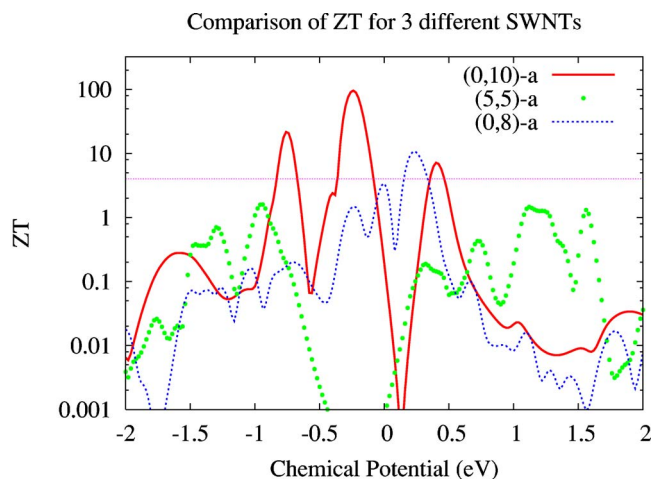


FIG. 2. (Color online) Figures of Merit for one (5,5) metallic, and two (8,0) and (10,0) semiconducting contacts plotted as a function of the chemical potential. Although ZT for the metallic tubes is always less than 1, that of semiconducting tubes can easily exceed 4 (dotted horizontal line), especially near the actual Fermi level of the tubes which is zero in our case.

Simply speaking, the nanocontact can be viewed as a barrier in the transport of ballistic electrons in a quantum wire. Interference effects due to multiple reflections at the contact walls, therefore, strongly affect the transport and create the observed fluctuations in the conductance.

C. Thermopower

The variations of the thermopower for structures (0,10)-a and (0,10)-b are displayed in Fig. 4.

Both tubes display large values for S as large as $7k_B/e$. This is consistent with another calculation also finding very

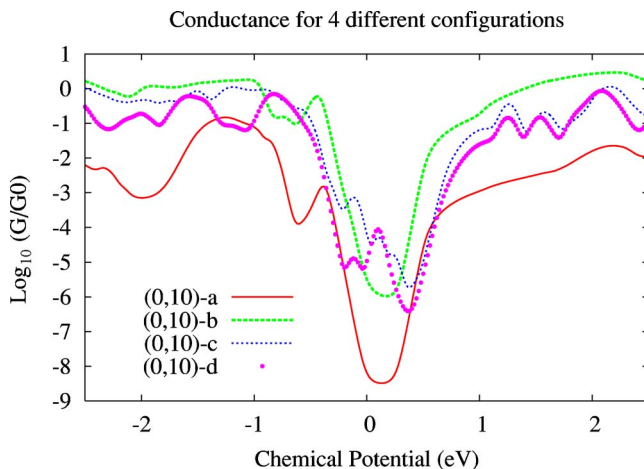


FIG. 3. (Color online) Log of the averaged conductance for the four separations (a)–(d), in units of $G_0 = 2e^2/h$ plotted as a function of the chemical potential. One can notice that the magnitude in case (a) is much reduced compared to (b) and others, meaning that the transport in (a) is tunneling dominated ($G \approx 0.01G_0$), whereas that in (b) is in the strong-coupling regime. The large conductance fluctuations as a function of the chemical potential and from sample to sample are due to quantum interferences.

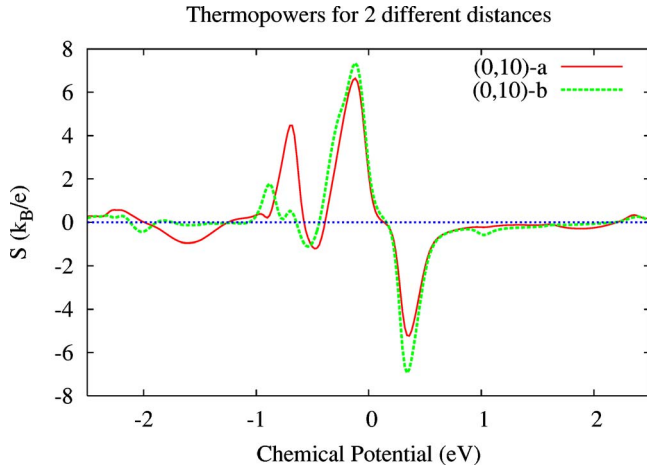


FIG. 4. (Color online) Seebeck coefficient for the two separations (a) and (b), in units of k_B/e plotted as a function of the chemical potential. One can notice the large fluctuations in the thermopower (due to mesoscopic conductance fluctuations), and its sign changes every time the conductivity is increasing and decreasing. For the sake of clarity only two typical curves are shown, but the thermopower of (c) and (d) also reach values near 7 and 5 k_B/e , respectively.

large values for the Seebeck coefficient of point contacts.¹⁸ Such large values have also been measured experimentally in 9 nm wires made of Bi/Al₂O₃.¹⁹ The actual chemical potential being equal to zero however, only values of S or σ or κ near $\mu=0$ are experimentally accessible. If hole- or electron-doped, the considered semiconducting tubes can achieve large thermopowers. As a comparison, standard semiconductors have $S < k_B/e$ and metals have $S \approx 0.01 k_B/e$. Therefore, this leads to a figure of merit which is a factor of almost 10 times larger compared to usual semiconductors, all other quantities assumed equal.

D. Wiedemann-Franz law

The other factor influencing the figure of merit is the Lorenz number: $\kappa/\sigma T$, which according to the Wiedemann-

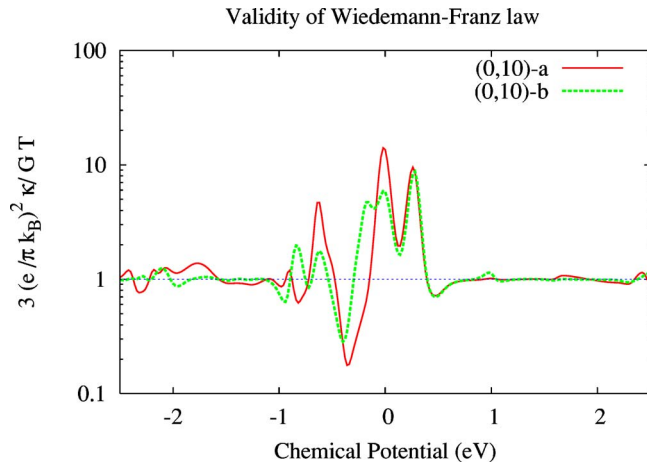


FIG. 5. (Color online) Logarithm of $3e^2/\pi^2 G k_B^2 T$ vs the chemical potential. Legends are similar to the figures.

Franz law is a constant for metals. In semiconductors, however, it can fluctuate as the Fig. 5 shows. The difference from 1 of the ratio $(3e^2/\pi^2 k_B^2)\kappa/GT$ shows a deviation from Wiedemann-Franz (WF) law. As can be seen in Fig. 5, this number varies from 0.2 to 10, and therefore, we can see large deviations from the WF law in semiconductor SWCNT contacts.

E. Figure of merit : ZT

Finally, the figure of merit of the four configurations is plotted versus the chemical potential in Fig. 6. One can see that near $\mu=0$ structure (0,10)-a can have figures of merit as large as 100! This can be traced back to a large thermopower in this energy range, and also a deviation from the WF law.

The advantage of this set up compared to other semiconducting thermoelectric devices is that the phonon contribution to the thermal conductivity, in the case where the separation is large, is presumably very small and thus the denominator in ZT does not need corrections and it remains small. It can also be seen that for all four configurations ZT can easily exceed 4 if the tubes are hole-doped. On the figure, the error bars for structure (0,10)-a are the error in mean, and since the average is over 50 configurations, the actual fluctuations in ZT is almost seven times larger than the error bars. One can conclude from this study, that for many arbitrarily chosen configurations the average figure of merit can by far exceeded 10.

F. Addition in series or parallel

One can ask what happens to the thermopower and the figure of merit, as such devices are added in series or in parallel. By this we mean a “classical” addition where interference effects do not come into play and between each of the two devices, thermal equilibrium is reached so that laws such as addition of resistances put in series, or conductances

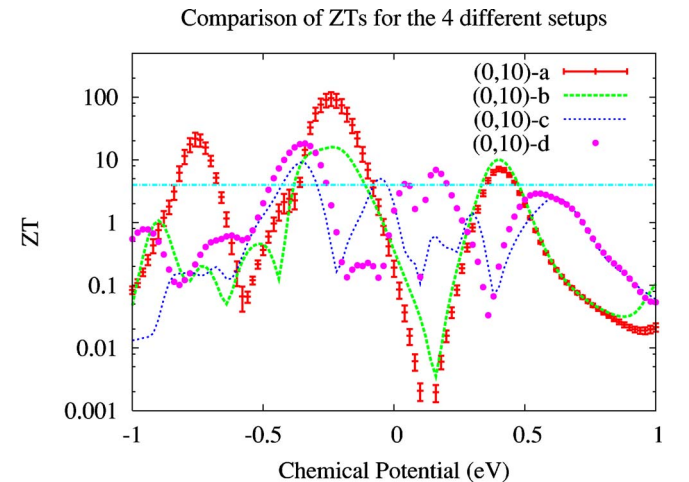


FIG. 6. (Color online) Figure of merit versus the chemical potential. For all configurations, it can reach values exceeding 10 just below the natural Fermi energy of the tubes. For the structure (a) the error bars are also shown. The dot-dashed line $ZT=4$ of conventional coolers is also drawn for comparison.

put in parallel apply. Otherwise the calculation becomes much involved as one has to include coherence effects. First let us discuss the Seebeck coefficient of N systems put in series and also in parallel. It can easily be shown from the definition of the transport coefficients that the Seebeck coefficient of N systems put in series is an average of the Seebeck coefficients weighted by their thermal resistance. Likewise, one can show that the equivalent Seebeck coefficient of N systems put in parallel is an average of the Seebeck coefficients weighted by their electrical conductance:

$$S_{\text{series}} = \frac{\sum_i S_i \rho_i^Q}{\sum_i \rho_i^Q} \quad (6)$$

$$S_{\text{parallel}} = \frac{\sum_i S_i G_i}{\sum_i G_i} \quad (7)$$

where ρ^Q is the thermal resistance.

In our proposed device, as can be seen from Fig. 3, the resistance for the hole doped case (μ just below 0), is of the order of $10^{+6} G_0^{-1} \approx 10^{+10} \Omega$ much larger than that of the leads. The thermal resistance is likewise orders of magnitude larger than that of the leads, implying that the measured Seebeck coefficient of such devices put in series is not affected by the presence of the leads at all since the thermal resistance of the latter is negligible. Moreover, if the devices are more or less identical, the total Seebeck coefficient is that of a single device.

Likewise, for M devices put in parallel, the equivalent Seebeck coefficient is identical to that of each individual device if they are all identical.

Now consider N identical devices put in series and M of those series put in parallel in order to be able to handle large surface areas (have a larger power factor) and large temperature and voltage gradients. The Seebeck of the whole system would be unchanged, and the electrical and thermal resistances are only scaled by N/M , therefore, the figure of merit would be the same as that of a single device. The study of statistical effects on the resulting thermopower and figure of merit are under investigation and will be discussed elsewhere.

IV. CONCLUSIONS

To summarize, we have shown that for semiconducting nanotube contacts large thermopowers and figures of merit can be achieved. The reason is twofold: Semiconducting nanotubes, if slightly doped, will have a strongly varying DOS near the chemical potential. This is a very important factor in producing large thermopowers. The second reason is the additional modulations of $T(E)$ due to the contact which can be viewed as a potential barrier. This leads to an oscillating transmission coefficient, present in all mesoscopic systems, due to interference effects. The combination of the two has yielded a strongly varying transmission and hence conductance as a function of the chemical potential (Fig. 3).

As a result of the mesoscopic nature of the device, the presence of impurities or a gate near the contact can strongly affect the interference patterns. This can be taken advantage of by tuning transport properties with a nanogate.

There are some simplifying assumptions and approximations in this model. Namely it is a one π orbital per carbon calculation of the coherent conductance neglecting the electron-phonon interaction and electron correlations beyond mean field. Also, in the calculation of ZT , we have neglected the thermal conductivity of the phonons, as the contact barely exists between the two nanotubes. We believe, based on the present calculations, however, that large values for the Seebeck coefficient ($S > 5k_B/e$) and also the figure of merit ($ZT > 10$) can be achieved in such systems; and as we showed, these features are quite robust with respect to atomic vibrations and different orientations of the two tubes. The present calculation is a proof of the concept. In an actual device, several such setups might be needed to be put in parallel and series in order to achieve reasonable amount of cooling. Having fluctuating values of σ , S , and κ from contact to contact, the overall performance will be affected, but our point here is just that a single ballistic contact can have large S and σ/κ at the same time; leading to ZT exceeding 10. The experimental realization of the proposed device might not be very easy, but we believe that other similar setups made of semiconducting ballistic quantum wire contacts will also display similar properties as the work by Hsu *et al.*⁴ on granular metals in a semiconductor matrix is already a witness to it. In their case, one is also in the tunneling regime, but presumably the contribution of the matrix phonons to the thermal conductivity brings down the figure of merit of the device. Another instance where such contacts can be made, is nano-peapods where one can easily insert fullerenes inside a nanotube. In this case, as the conduction needs to take place through the buckyballs, the nanotube should be of large bandgap. Boron-Nitride nanotubes are thus a good candidate for holding the buckyballs. The series of buckyballs have the extra effect of energy filtering similar to superlattices. In general, we believe that any percolated path of electrons hopping through granular metals embedded in a semiconducting matrix, has the potential of displaying large thermopowers easily exceeding k_B/e . In order to achieve large ZT , one additionally needs to have a very low thermal conductivity. This can be achieved if the thermal wavelength of the phonons is of the order of their mean free path or less.

ACKNOWLEDGMENTS

We would like to thank Dr. A. Shakouri for suggesting this problem and useful discussions, as well as Dr. A. A. Farajian for discussions and a critical reading of the manuscript. K.E. would also like to acknowledge the Iranian Ministry of Science and Technology for financial support, and the Japanese Society for Promotion of Science (JSPS) for funding his trip to the Institute for Materials Research where part of this work was done.

- ¹G. D. Mahan, *J. Appl. Phys.* **76**, 4362 (1994); G. D. Mahan, *Solid State Physics* (Academic, New York, 1998), Vol. 51, p. 81.
- ²L. D. Hicks and M. S. Dresselhaus, *Phys. Rev. B* **47**, 12727 (1993); **47**, 16631 (1993).
- ³X. Sun, Z. Zhang, and M. S. Dresselhaus, *Appl. Phys. Lett.* **74**, 4005 (1999).
- ⁴K. F. Hsu, S. Loo, F. Guo, W. Chen, J. S. Dyck, C. Uher, T. Hogan, E. K. Polychroniadis, and M. G. Kanatzidis, *Science* **303**, 818 (2004).
- ⁵R. Venkatasubramanian, E. Siivola, T. Colpitts, and B. O'Quinn, *Nature (London)* **413**, 597 (2001).
- ⁶H.-K. Lyeo, A. A. Khajetoorians, L. Shi, K. P. Pipe, R. J. Ram, A. Shakouri, and C. K. Shih, *Science* **303**, 816 (2004).
- ⁷J. Hone, I. Ellwood, M. Muno, A. Mizel, M. L. Cohen, A. Zettl, A. G. Rinzler and R. E. Smalley, *Phys. Rev. Lett.* **80**, 1042 (1998); W. Zhou, J. Vavro, N. M. Nemes, J. E. Fischer, F. Borondics, K. Kamaras, D. B. Tanner, *Phys. Rev. B* **71**, 205423 (2005) and references therein.
- ⁸C. Park, Z. Ounaies, K. A. Watson, R. E. Crooks, J. Smith, Jr., S. E. Lowther, J. W. Connell, E. J. Siochi, J. S. Harrison, and T. L. St. Clair, *Chem. Phys. Lett.* **364**, 303 (2002); B. E. Kilbride, J. N. Coleman, J. Fraysse, P. Fournet, M. Cadec, A. Drury, S. Hutzler, S. Roth, and W. J. Blau, *J. Appl. Phys.* **92**, 4024 (2002).
- ⁹M. Baxendale, K. G. Lim, and G. A. J. Amaratunga, *Phys. Rev. B* **61**, 12705 (2000).
- ¹⁰M. Foygel, R. D. Morris, D. Anez, S. French, and V. L. Sobolev, *Phys. Rev. B* **71**, 104201 (2005).
- ¹¹J. P. Small, K. M. Perez, and P. Kim, *Phys. Rev. Lett.* **91**, 256801-1 (2003).
- ¹²P. J. Lin-Chung and A. K. Rajagopal, *Phys. Rev. B* **65**, 113408 (2002).
- ¹³R. Landauer, *IBM J. Res. Dev.* **1**, 233 (1957).
- ¹⁴M. Buttiker, Y. Imry, R. Landauer, and S. Pinhas, *Phys. Rev. B* **31**, 6207 (1985); M. Buttiker, *Phys. Rev. Lett.* **57**, 1761 (1986); *IBM J. Res. Dev.* **32**, 317 (1988).
- ¹⁵H. M. Pastawski, *Phys. Rev. B* **44**, 6329 (1991); Y. Meir and N. S. Wingreen, *Phys. Rev. Lett.* **68**, 2512 (1992); S. Datta, *Electronic Transport in Mesoscopic Systems* (Cambridge University Press, 1995).
- ¹⁶N. W. Ashcroft and N. D. Mermin, *Solid State Physics* (Holt, Rinehart and Winston, New York, 1976).
- ¹⁷U. Sivan and Y. Imry, *Phys. Rev. B* **33**, 551 (1986).
- ¹⁸C. W. J. Beenakker and A. A. M. Staring, *Phys. Rev. B* **46**, 9667 (1992).
- ¹⁹J. P. Heremans, C. M. Thrush, D. T. Morelli, and M. C. Wu, *Phys. Rev. Lett.* **88**, 216801 (2002).